

# On the use of 2D correlation and exchange NMR spectroscopy in organic porous materials

Petrik Galvosas<sup>a,b,\*</sup>, Ying Qiao<sup>b</sup>, Monika Schönhoff<sup>c</sup>, Paul T. Callaghan<sup>b</sup>

<sup>a</sup>Faculty of Physics and Earth Sciences, University of Leipzig, D-04103 Leipzig, Germany

<sup>b</sup>MacDiarmid Institute for Advanced Materials and Nanotechnology, SCPS, Victoria University of Wellington, 6005 Wellington, New Zealand

<sup>c</sup>Institut für Physikalische Chemie, Westfälische Wilhelms-Universität Münster D-48149 Münster, Germany

---

## Abstract

Two-dimensional (2D) nuclear magnetic resonance (NMR) methods for the investigation of correlation and exchange have been introduced in recent years and have been applied to a range of different systems. Here, we report on the use of 2D NMR diffusion–diffusion correlation spectroscopy for the investigation of diffusion anisotropy in cellular plant tissues and of diffusion–diffusion exchange spectroscopy for the study of the diffusive exchange of dextran in a dispersion of polyelectrolyte multilayer hollow capsules. Furthermore, diffusion–relaxation correlation spectroscopy was applied to both systems.

© 2007 Elsevier Inc. All rights reserved.

*Keywords:* 2D NMR; Inverse Laplace transformation; Diffusion; Exchange; Anisotropy

---

## 1. Introduction

Besides the established multidimensional methods of nuclear magnetic resonance (NMR) spectroscopy for the study of complex systems (e.g., see Ernst et al. [1]), recent methods have become available with the introduction of data analysis algorithms suitable for PC. Namely, the algorithm suggested in Venkataramanan et al. [2] enables one to perform two-dimensional (2D) inverse Laplace transformation without the need for super computers. Since its introduction and first application [3], a growing number of experiments and applications have been found in the literature (e.g., see Callaghan et al. [4], Stallmach and Galvosas [5] and Callaghan et al., this issue). In this article, we report on the use of three 2D NMR experiments, each involving an inverse Laplace transformation and application to two porous materials. While diffusion–diffusion correlation spectroscopy (DDCOSY) is used for the characterization of anisotropic diffusion in plant tissues, diffusion exchange spectroscopy [diffusion–diffusion exchange spectroscopy (DEXSY)] is employed for the investigation of dextran exchange between the interior and the exterior of

hollow polyelectrolyte multilayer (PEM) capsules. Furthermore, diffusion–relaxation correlation spectroscopy (DRCOSY) is applied to both systems. Although results have been published previously [6,7], here we summarize the main features of the 2D inverse Laplace approach and shed light onto corresponding experiments utilizing pulsed field gradient (PFG) NMR.

DEXSY [4,8] employs two successive PFG NMR sequences [9] separated by a mixing time  $\tau_m$ , in which collinear gradient pairs  $G_1$  and  $G_2$  may be varied independently (Fig. 1). Therefore, acquired NMR signal is a function of applied gradients, which, using the wave vector  $q = \gamma \delta g$ , lead to:

$$\frac{M(q_1^2, q_2^2)}{M_0} = \sum p(D_1, D_2) e^{-q_1^2 D_1 \Delta} e^{-q_2^2 D_2 \Delta}, \quad (1)$$

where  $M$  is the echo amplitude,  $M_0$  is the initial echo amplitude,  $\Delta$  is the observation time and  $p$  is the joint probability of contribution to the signal from diffusion coefficients  $D_1$  and  $D_2$ .  $G$ ,  $\gamma$  and  $\delta$  are the gradient strength, gyromagnetic ratio and gradient duration, respectively. Eq. (1) is a discrete representation of a 2D Laplace integral. Therefore, if  $M$  is subjected to an inverse Laplace transformation, one can determine the probability  $p$  from the experiment. For DEXSY, this leads to a 2D map of

---

\* Corresponding author. Fax: +49 341 9732549.

E-mail address: [galvosas@physik.uni-leipzig.de](mailto:galvosas@physik.uni-leipzig.de) (P. Galvosas).

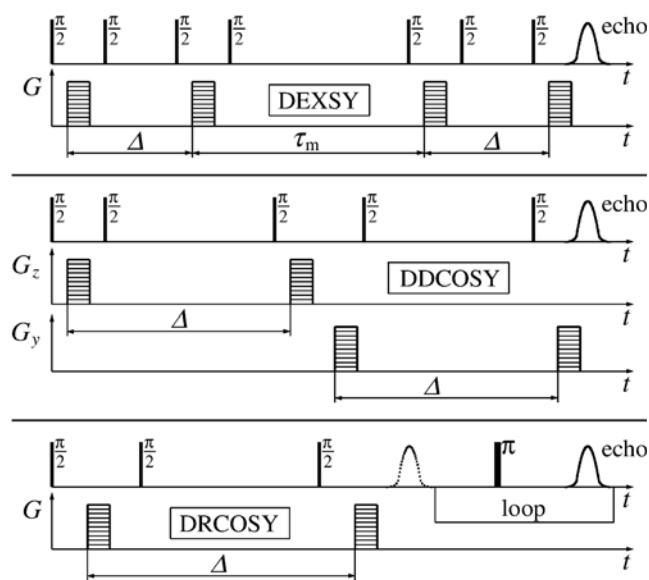


Fig. 1. The DEXSY pulse sequence consists of two collinear gradient pairs separated by mixing time  $\tau_m$ . In contrast, DDCOSY uses two gradient pairs, which may be collinear (not shown) or orthogonal. DRCOSY combines a pulsed gradient stimulated echo (PGSTE) sequence with a Carr-Purcell-Meiboom-Gill (CPMG) sequence. All gradient pulses have a width  $\delta$ .

diffusion coefficients in which diagonal peaks represent molecules with the same  $D$  before and after  $\tau_m$ . On the contrary, if exchange processes involve a change of  $D$  during  $\tau_m$ , corresponding off-diagonal peaks appear on the 2D map.

DDCOSY [4,8] also employs two PFG NMR sequences. In contrast to DEXSY,  $\tau_m$  is chosen to be minimal (Fig. 1). Furthermore, independent gradient pairs  $G_i$  and  $G_j$ , with  $i$  and  $j$  equal to  $x$ ,  $y$  or  $z$ , may be applied collinearly or orthogonally to correlate successive diffusion along the corresponding axis of the laboratory frame of reference.

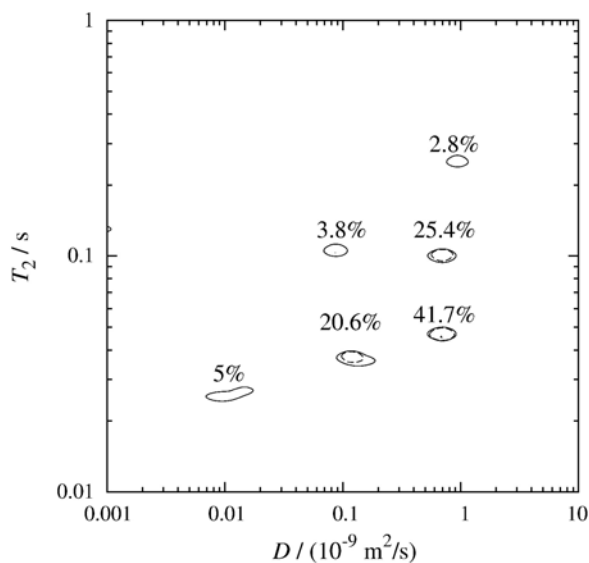


Fig. 2. DRCOSY of the chive sample at  $\Delta=300$  ms. Contour levels are placed at 1%, 10% and 100% of the highest peak.

Therefore, the signal is a function of applied gradients, leading to:

$$\frac{M(q_i^2, q_j^2)}{M_0} = \sum p(D_{ii}, D_{jj}) e^{-q_i^2 D_{ii} \Delta} e^{-q_j^2 D_{jj} \Delta}, \quad (2)$$

where  $p$  is the joint probability of contribution to the signal from tensor elements  $D_{ii}$  and  $D_{jj}$ . Similar to DEXSY, an inverse Laplace transformation of experimental data  $M$  from Eq. (2) provides a 2D map of diffusion tensor elements in the corresponding spatial directions. Isotropic diffusion behavior is represented by diagonal peaks of the map, while off-diagonal peaks appear when the diffusion coefficient is a tensor.

DRCOSY [10] uses a PFG NMR pulse sequence combined with a CPMG sequence [11]. In contrast to DRCOSY published in Godefroy and Callaghan [10], here, a multi-echo sampling Carr-Purcell-Meiboom-Gill (CPMG) sequence is used (Fig. 1). Therefore, the resulting signal, represented by the maximum of each successive echo in the time domain, is given by:

$$\frac{M(q^2, t)}{M_0} = \sum p(D, T_2) e^{-q^2 D \Delta} e^{-t/T_2}, \quad (3)$$

where  $p$  is the joint probability of contribution to the signal from  $D$  and  $T_2$ . Again, inverse Laplace transformation, when applied to experimental data  $M$ , unfolds a 2D map in which individual peaks correlate diffusion coefficients with the corresponding  $T_2$ .

## 2. Experimental

Plant tissues were taken from living chive leaves (*Allium schoenoprasum*). In order to study diffusion anisotropy even in the case of a globally homogeneous sample, the

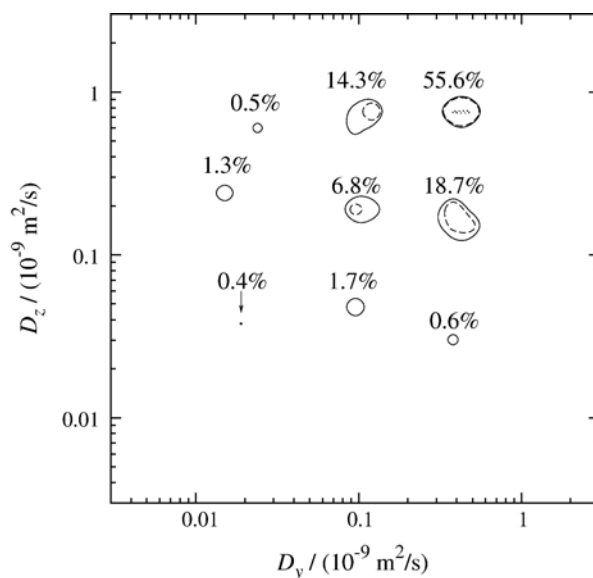


Fig. 3. DDCOSY of the chive sample at  $\Delta=300$  ms. Contour levels are placed at 1%, 10% and 100% of the highest peak.

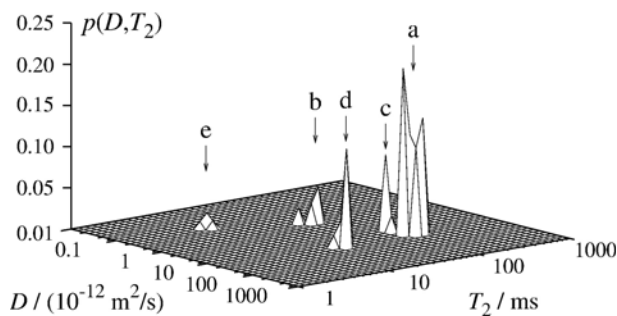


Fig. 4. DRCOSY of dextran (see text for details).

leaves were chopped into cylindrical pieces of about 2–5 mm and filled into a 20 mm sample tube. In this way, a powder-like sample was prepared with random orientation of leaf pieces (see Qiao et al. [7]).

The capsule system consists of dextran (77 kDa, 3.3 mg/ml) in a dispersion of PEM capsules (four layers of polystyrene sulfonate/polydiallyldimethylammonium chloride (PSS/PDADMAC); diameter 520 nm) with a volume ratio of 10% vol/vol in D<sub>2</sub>O (see Qiao et al. [6] and Adalsteinsson et al. [12]).

Experiments were performed using a Bruker AMX 300 NMR spectrometer at a <sup>1</sup>H resonance frequency of 300.14 MHz at room temperature. The gradients were generated either with a Bruker Micro 2.5 (the maximum gradient employed was 0.937 T/m) or with a Bruker Diff 60 (the maximum gradient employed was 9.12 T/m), depending on the smallest diffusion coefficient to be measured. The parameters for inverse Laplace transformation were chosen according to Venkataramanan et al. [2]. Limits in *D* and *T*<sub>2</sub> domains are indicated by axes in Figs. 2–5 and the regularization parameter  $\alpha = 10^{12} - 10^{13}$ . The signal-to-noise ratio is between 30 and 50 dB for all data sets.

### 3. Results and discussion

DRCOSY at  $\Delta = 300$  ms in Fig. 2 represents distinct properties of water in respect to its diffusivity and *T*<sub>2</sub> in different sites of the chive tissue. We note that inverse Laplace transformation tends to collect intensity into discrete peaks even in cases of continuous distributions (i.e., pearling effect; see Callaghan et al. [4] and Callaghan and Furo [8]). For further interpretation, we involve results from DDCOSY, as shown in Fig. 3. Diagonal peaks are roughly separated by one order of magnitude and agree with the three groups in the diffusion dimension of Fig. 2.

Three pairs of corresponding off-diagonal peaks exist in Fig. 3. The first pair with 0.5% and 0.6% can be attributed to diffusion in xylem vessels because of their strong anisotropy. This pair corresponds to the peak with 2.8% (because of long *T*<sub>2</sub> and small probability) and 5% (because of *D*) on the DRCOSY map. A second pair can be found with 14.3% and 18.7%. The fast component of the diffusion tensor corresponds to peaks with 25% and 41.7% on the DRCOSY map (Fig. 2), while its slow component corre-

sponds to peaks with 3.8% and 20.6%. All four peaks on the DRCOSY map have a much smaller *T*<sub>2</sub> compared to water in xylem vessels, and diffusion is more restricted even for the fast component. Moreover, it involves most of the water within cell tissues. This suggests diffusion in palisade and spongy mesophyll cells, which occupy most cellular tissues. These cells are either isodiametric (supporting the large isotrope peak with 55.6% in Fig. 3) or elongated along the radial axis (represented by peaks with 14.3% and 18.7%). The third pair with 1.3% and 1.7% could be explained by the diffusion of intercellular water because of its very small diffusion coefficient, which is about one and two orders below the diffusion of bulk water.

DRCOSY with  $\Delta = 60$  ms to 300 ms was used for the investigation of the time dependence of dextran diffusion and relaxation in capsule dispersion. Fig. 4 is an example of  $\Delta = 100$  ms. A detailed analysis of the capsule system with DRCOSY is contained in Qiao et al. [6]; here, we merely summarize key results.

Peaks (a) and (d) correspond to the diffusion of free dextran with  $D_{\text{free}} = 2.5 \times 10^{-11}$  m<sup>2</sup>/s, while Peak (b) represents dextran confined inside individual capsules, with measures of their diffusion coefficient ( $D_{\text{conf}}$ ). The latter slightly decreases and settles at  $\approx 6 \times 10^{-13}$  m<sup>2</sup>/s at  $\Delta = 150$  ms, which is consistent with a model of hard spheres in a free volume. It is easy to show that Peak (c) cannot arise from dextran in a fast exchange between the free phase and a confined phase. Instead, we suggest that free dextran molecules temporarily interact ( $D_{\text{int}} = 1.1 \times 10^{-11}$  m<sup>2</sup>/s) with the surface of capsules and rejoin the free phase on a time scale shorter than  $\Delta$ . Eventually, Peak (e) arises from dextran trapped inside hollow capsule clusters. Most remarkably, most of dextran ( $\approx 70\%$ ) is confined in or

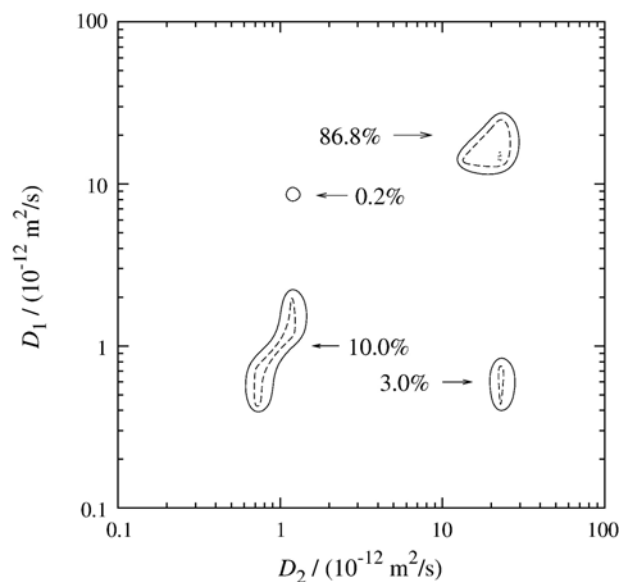


Fig. 5. Diffusion exchange of dextran between the interior of the capsules and the free solution for  $\tau_m = 200$  ms. Contour levels are placed at 0.01%, 1% and 100% of the highest peak.

attached to these clusters and individual capsules, hence being concentrated in a volume of only  $\approx 10\%$  of the sample. We estimated an enhancement factor up to about 30 and confirm the existence of this effect, which was first reported in Adalsteinsson et al. [12].

DEXSY with  $\tau_m=200$  ms and  $\Delta=60$  ms only measures Peaks (a), (b) and (c) due to relaxation time weighting. In Fig. 5, therefore, diagonal peaks correspond to  $D_{\text{conf}}$  (10%) and  $D_{\text{free}}$  joined with  $D_{\text{int}}$  (86%). The intensities of these peaks match those extracted from DRCOSY for Peaks (a)–(c) only. However, the most intriguing feature in Fig. 5 is the presence of off-diagonal peaks, providing evidence for dextran exchange between the interior and the exterior of the capsules — a feature that does not appear for  $\tau_m=20$  ms (figure not shown).

Obviously, as required by thermal equilibrium, we have to attribute the intensity imbalance of off-diagonal peaks to experimental errors. In contrast, the position asymmetry of off-diagonal peaks may not arise from uncertainties. We propose that dextran molecules, which are initially confined in capsules, may eject directly into the free dextran phase, as suggested by the peak with 3%. On the contrary, dextran, which joins confinement in the capsule during  $\tau_m$ , exhibits a diffusion coefficient close to  $D_{\text{int}}$ , as given by the peak with 0.2%. We therefore postulate that only dextran, which temporarily interacts with the outer surface of the capsule, may enter its interior.

#### 4. Conclusions

In this article, we summarized two applications of recent 2D NMR correlation and exchange methods. We focused on how 2D Laplace inversion can provide a detailed insight on complex porous systems.

DRCOSY and DDCOSY enable one to characterize water sites in cellular tissues of chopped chive leaves. While DRCOSY discriminates sites by diffusion restriction and  $T_2$ , DDCOSY correlates corresponding diffusion tensor elements. The joint interpretation of both methods allows one to assign various water peaks to cell shapes and orientations at a size scale beyond the resolution of standard NMR microscopy methods.

DRCOSY and DEXSY were used to investigate the time dependence and exchange of dextran diffusion in a dispersion of PEM hollow capsules. While DRCOSY at

different  $\Delta$  values allows one to discriminate different diffusion modes of dextran and to estimate dextran enhancement (about 30) within capsules and capsule clusters, DEXSY exhibits an exchange of about 1.5% of dextran at  $\tau_m=200$  ms, suggesting an exchange time on the order of  $\approx 1$  s.

#### Acknowledgments

We gratefully acknowledge financial support provided by the New Zealand Centers of Research Excellence Fund; the New Zealand Foundation for Research, Science and Technology; and the Royal Society of New Zealand Marsden Fund. We thank Thorsteinn Adalsteinsson for the preparation of PEM capsule samples.

#### References

- [1] Ernst RR, Bodenhausen G, Wokaun A. Principles of nuclear magnetic resonance in one and two dimensions. Oxford: Clarendon Press; 1987.
- [2] Venkataramanan L, Song YQ, Hürlimann MD. Solving Fredholm integrals of the first kind with tensor product structure in 2 and 2.5 dimensions. IEEE Trans Signal Process 2002;50(5):1017–26.
- [3] Song YQ, Venkataramanan L, Hürlimann MD, Flaum M, Frulla P, Straley C.  $T_1$ – $T_2$  correlation spectra obtained using a fast two-dimensional Laplace inversion. J Magn Reson 2002;154:261–8.
- [4] Callaghan PT, Godefroy S, Ryland BN. Use of the second dimension in PGSE NMR studies of porous media. Magn Reson Imaging 2003;21(3–4):243–8.
- [5] Stallmach F, Galvosas P. Spin echo NMR diffusion studies. Annu Rep NMR Spectrosc, vol. 61. Elsevier; 2007 [in press].
- [6] Qiao Y, Galvosas P, Adalsteinsson T, Schönhoff M, Callaghan PT. Diffusion exchange NMRs spectroscopic study of dextran exchange through polyelectrolyte multilayer capsules. J Chem Phys 2005; 122:214912.
- [7] Qiao Y, Galvosas P, Callaghan PT. Diffusion correlation NMR spectroscopic study of anisotropic diffusion of water in plant tissues. Biophys J 2005;89(4):2899–905.
- [8] Callaghan PT, Furo I. Diffusion–diffusion correlation and exchange as a signature for local order and dynamics. J Chem Phys 2004; 120(8):4032–8.
- [9] Tanner JE. Use of the stimulated echo in NMR diffusion studies. J Chem Phys 1970;52:2523.
- [10] Godefroy S, Callaghan PT. 2D relaxation/diffusion correlations in porous media. Magn Reson Imaging 2003;21:381–3.
- [11] Meiboom S, Gill D. Modified spin-echo method for measurement of relaxation times. Rev Sci Instrum 1958;29:688–91.
- [12] Adalsteinsson T, Dong WF, Schönhoff M. Diffusion of 77000 g/mol dextran in submicron polyelectrolyte capsule dispersions measured using PFG-NMR. J Phys Chem B 2004;108(52):20056–63.